Available online at www.sciencedirect.com

SciVerse ScienceDirect

journal homepage: www.elsevier.com/locate/jmbbm

Research Paper

Bio-inspired interfacial strengthening strategy through geometrically interlocking designs

Yuming Zhang[a,b,1], Haimin Yao[c,*,1], Christine Ortiz[b], Jinquan Xu[a], Ming Dao[b,*]

[a]Department of Engineering Mechanics, Shanghai Jiaotong University, Shanghai 200240, China
[b]Department of Materials Science and Engineering, Massachusetts Institute of Technology, 77 Massachusetts Avenue, Cambridge, MA 02139, USA
[c]Department of Mechanical Engineering, The Hong Kong Polytechnic University, Hung Hom, Kowloon, Hong Kong SAR, China

ARTICLE INFO

ABSTRACT

Many biological materials, such as nacre and bone, are hybrid materials composed of stiff brittle ceramics and compliant organic materials. These natural organic/inorganic composites exhibit much enhanced strength and toughness in comparison to their constituents and inspires enormous biomimetic endeavors aiming to synthesize materials with superior mechanical properties. However, most current synthetic composites have not exhibited their full potential of property enhancement compared to the natural prototypes they are mimicking. One of the key issues is the weak junctions between stiff and compliant phases, which need to be optimized according to the intended functions of the composite material. Motivated by the geometrically interlocking designs of natural biomaterials, here we propose an interfacial strengthening strategy by introducing geometrical interlockers on the interfaces between compliant and stiff phases. Finite element analysis (FEA) shows that the strength of the composite depends strongly on the geometrical features of interlockers including shape, size, and structural hierarchy. Even for the most unfavorable scenario when neither adhesion nor friction is present between stiff and compliant phases, the tensile strength of the composites with proper interlocker design can reach up to 70% of the ideal value. The findings in this paper would provide guidelines to the improvement of the mechanical properties of current biomimetic composites.

© 2012 Elsevier Ltd. All rights reserved.

1. Introduction

In nature, the structure of "staggered hard crystals embedded in soft matrix" (Fratzl and Jager, 2000) is widely observed in biomineralized tissues such as nacre, bone and tooth. As a metaphor, it is often referred to as "brick-and-mortar" (B-and-M) structure. These structural (load-bearing) biocomposites generally contain a multitude of interfaces between stiff and compliant constituents (phases) at multiple length scales (Dunlop and Fratzl, 2010; Ortiz and Boyce, 2008; Ritchie, 2011; Weiner et al., 2006; Yao et al., 2010). Here interface is defined as the area between two condensed phases (Geckeler et al., 1997). Recently, attention has been drawn that natural biomineralized tissues achieve a balance between strength

and toughness by means of B-and-M structure. On the one hand, the unique geometry and spatial arrangement of the microscopic stiff phases compensates the low strength of the compliant phase (Ji and Gao, 2004; Wang et al., 2001). On the other hand, toughening mechanisms such as plastic yielding of compliant phase, microcracking and crack bridging, and pulling-out of stiff phase from compliant phase would cause more energy dissipation and hence lead to higher toughness of the biocomposites (Gao et al., 2003; Launey et al., 2010; Nalla et al., 2004; Tai et al., 2007; Yao et al., 2011). The ever-increasing knowledge of the strengthening and toughening mechanisms of these hierarchical structural biocomposites has inspired the advent of a variety of man-made biomimetic materials (Bonderer et al., 2008; Munch et al., 2008; Podsiadlo et al., 2007; Tang et al., 2003). For instance, Bonderer et al. adopted sub-micrometer-thick ceramic platelets and ductile polymer matrix to fabricate layered hybrid films (Bonderer et al., 2008). Munch et al. emulated the nacre structure by hybridizing aluminum oxide and polymethyl mechacrylate into ice-templated structures, resulting in a composite with

much enhanced toughness (Munch et al., 2008). Despite of these achievements, the potential of the biomimetic artificial composites has not been exploited fully due to the insufficiency of brick/mortar interface which plays an eminent role in load transferring (Podsiadlo et al., 2007; Rexer and Anderson, 1979; Schmidt et al., 2002). Indeed, the mechanical performances of B-and-M biocomposites are critically dependent on the mechanical properties of the interface. For example, the tensile strength is determined by the weakest term among the interface strength, the yield strength of the compliant layer and the strength of the stiff phase (Gao, 2006). To strengthen the interface, one of the effective ways that nature adopts in biocomposites is making use of interface roughness at several length scale levels. Existing examples include the nano-asperities on the aragonite tablets in nacre (Han et al., 2011; Wang et al., 2009, 2001), interdigitated morphology of cranial joints (Herring, 2008; Jasinoski et al., 2010), and the hierarchical interlocking between functional layers of a snail shell shown in Fig. 1a. Studies on the effect of such interfacial roughness on the mechanical properties of
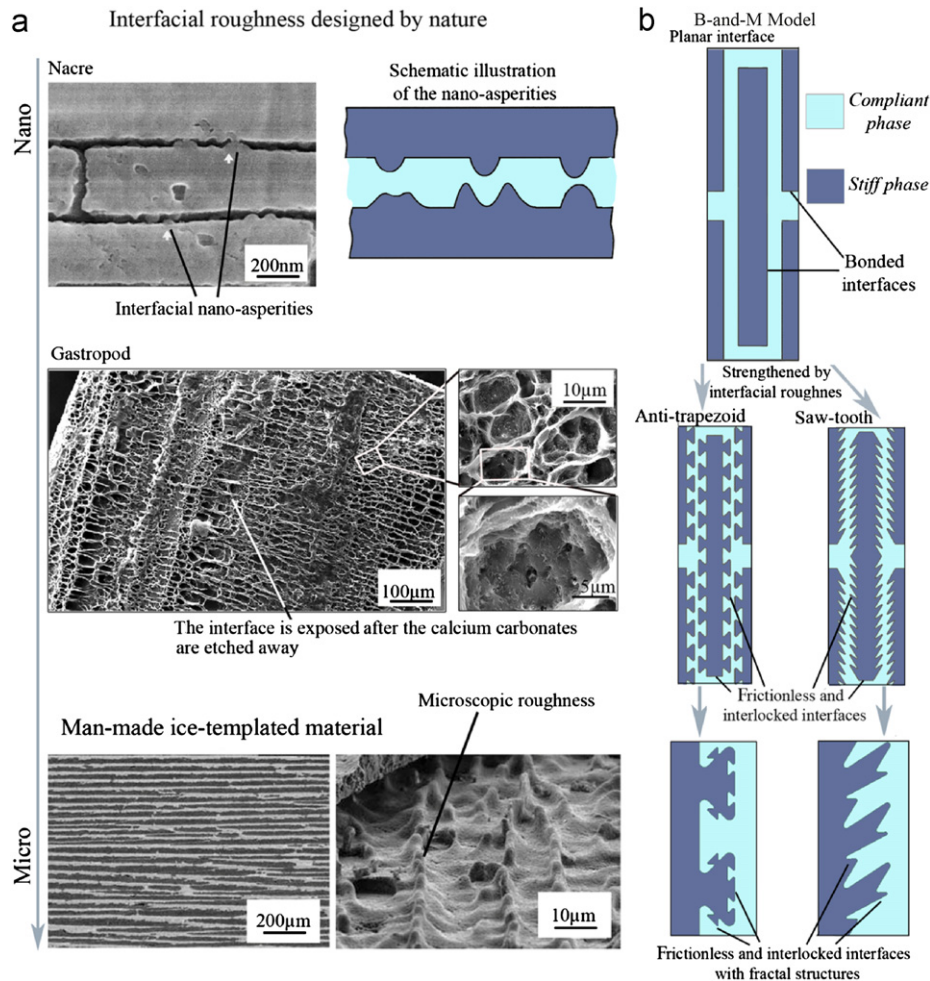

Fig. 1 – Interfacial interlocking designs adopted in natural and synthetic B-and-M composites. (a) The interfacial interlocking designs at different length scales in natural materials. Top: the nanoasperities on aragonite surface in nacre (Wang et al., 2001) (reprinted with permission); middle: the organic layer surface exposed after removal of the adjacent mineral layer by etching (Yao et al., 2010); bottom: the bumpy interface in a layered synthetic composite (Munch et al., 2008) (reprinted with permission). (b) Schematics of the original (plain) B-and-M model (top), modified B-and-M structure with interfacial interlocker (middle), and modified B-and-M structure with fractal interfacial interlocker designs (bottom).

the related biological structural systems were carried out. It was found that the nano-asperities on the aragonite tablets in nacre would increase the contact area between organic and inorganic materials, resulting in higher magnitude of plastic strains after yield (Katti et al., 2004), while the morphology of the interdigitation of cranial bones was found to play an important role in determining the mechanical properties of the suture joints (Li et al., 2011, 2012). But so far the quantitative knowledge of the effect of interface strength on the mechanical performance of B-and-M composites is still deficient. Inspired by nature with its use of geometrical interlocking to optimize the mechanical properties of interfaces (Hammer and Tirrell, 1996), in this paper we theoretically explore the effect of interfacial interlocking structures on the tensile strength of B-and-M composites by using finite element modeling. The rest of this paper is planned as follows. First, the computational models are introduced briefly. Then parametric studies are conducted to investigate the effect of geometric factors of the interlocking design on the tensile strength, followed by the discussion on the potential applications of our results. Finally, the paper is concluded with summary of present study and outlook of future work.

2.   Model

Based on the interfacial interlocking observed in the natural prototypes and their synthetic mimics (see Fig. 1a) (Jasinoski et al., 2010; Krauss et al., 2009; Saunders, 1995; Yao et al., 2010), two types of interfacial interlocker, including anti-trapezoid and saw-tooth, were considered. The modified two-dimensional B-and-M structures with incorporation of these two types of interlockers were adopted as our computational models, as shown in Fig. 1b. We took the aspect ratio of the stiff platelets $\rho \cong 10$ (Gao et al., 2003) and volume fraction of stiff phase $\Phi \cong 60\%$. The compliant and stiff phases were assumed as elastic-perfectly-plastic and elastic, respectively. While the Young's modulus of the stiff material was taken as 92 GPa (Gao, 2006), the shear modulus and tensile strength of the compliant material were chosen as 7 GPa and 20 MPa respectively (with the equivalent shear strength being 11.55 MPa based on the von Mises yield criterion). The Poisson's ratios of the stiff and compliant phases were taken as 0.3 and 0.4 (Liu et al., 2006) respectively. Finite element analysis (FEA) was conducted with a commercial FEA software ABAQUS (Dassault Systèmes, Providence, RI, USA) to calculate the strength under uniaxial tension along the longitudinal direction. Periodic boundary conditions were applied on both lateral sides of the computational models. Four-node bilinear plane strain quadrilateral element (CPE4R) was adopted in all simulations. We recognize that mechanisms other than geometrical interlocking (e.g. frictions and adhesions) also contribute to the tensile strength. In order to avoid these effects and assess the contribution of geometrically interlocking designs solely, contact between compliant and stiff materials were assumed as frictionless and non-adhesive except for the control cases, in which perfect (unbreakable) bonding and/or planar interfaces were considered for comparison.
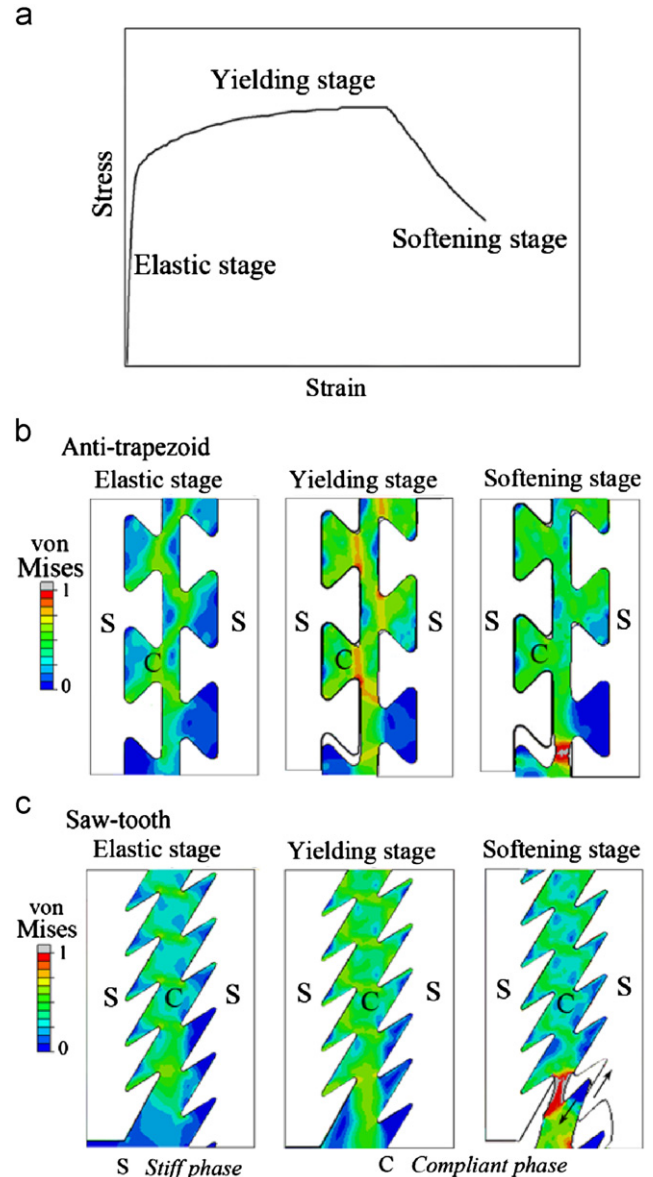

Fig. 2 – (a) A typical stress–strain curve of a B-and-M model with interfacial interlocking design under uniaxial tension. Snapshots of von Mises stress field in the compliant phase at different stages of deformation for (b) anti-trapezoid and (c) saw-tooth designs. The magnitude of stress here is normalized by the yield strength of the compliant phase, and the snapshots are taken when the loading reaches 70%, 100% and 70% (from the left to the right) of the maximum tensile strength of each model, respectively.

3.   Results

Fig. 2a shows a typical stress–strain curve obtained in our simulations. It can be seen that the deformation of B-and-M composites with interfacial interlocking design typically experiences three stages before final failure: elastic stage, yielding stage, and softening stage. In the elastic stage, the stress increases with the strain linearly. At a critical point of load, yielding occurs due to the yield of the compliant phase or the

separation between the stiff and compliant phases. With further extension, the loading stress increases gradually and eventually reaches a maximum point, beyond which the carrying capacity of the composites drops. After a period of softening, the failure of the composite takes place. Fig. 2 shows the snapshots of the von Mises stress at different stages of deformation. Unlike the perfect bonding case, in which the failure predicted by the FEA model always occurs through shear failure of the compliant phase, in the cases without perfect bonding failure may occur due to lateral unlocking of two phases or localized shear failure of compliant matrix.

The tensile strength, which is defined as the maximum sustainable tensile stress of a material, is one of the important mechanical properties. In our modeling, our results indicate that calculated tensile strength σ_{pb} for the perfect bonding case is 36.6 MPa and varies little with the geometry of interlocker structures. This value agrees well with the theoretical estimation of 38.5 MPa by a simpler theoretical model assuming that the compliant material sustains no tension but shear loading only (Gao, 2006). We thus defines $\sigma_{pb}=36.6$ MPa as the ideal strength of the composite under consideration and employ it to benchmark the strengthening effect of various interlocking designs in the following. It is noteworthy that for a planar interface without adhesion and friction, the composite retains vanishing tensile strength.

3.1. Strengthening effects of the anti-trapezoid design

For the anit-trapezoid case, we began with the investigation into the effect of its shoulder width w on the tensile strength. We kept the height (h) and volume of anti-trapezoid as constants, as shown in Fig. 3a. The calculated variation of tensile strength as a function of shoulder width is shown in Fig. 3b. It is interesting to notice that neither smaller nor larger shoulder width would lead to higher tensile strength. There is an optimal ratio of w/h, at which the tensile strength is maximized. This phenomenon can be elucidated by comparing the stress and deformation in different cases, as shown in Fig. 3c. If the volume of the anti-trapezoid is maintained constant, larger shoulder width gives rise to smaller neck width, which is defined as the shorter base of the anti-trapezoid. Plastic yielding occurs easily in the interlocker with smaller neck width, leading to localized interlocker failure and thereby lower tensile strength. On the other hand, if the shoulder width is too small, the mechanical interlocking
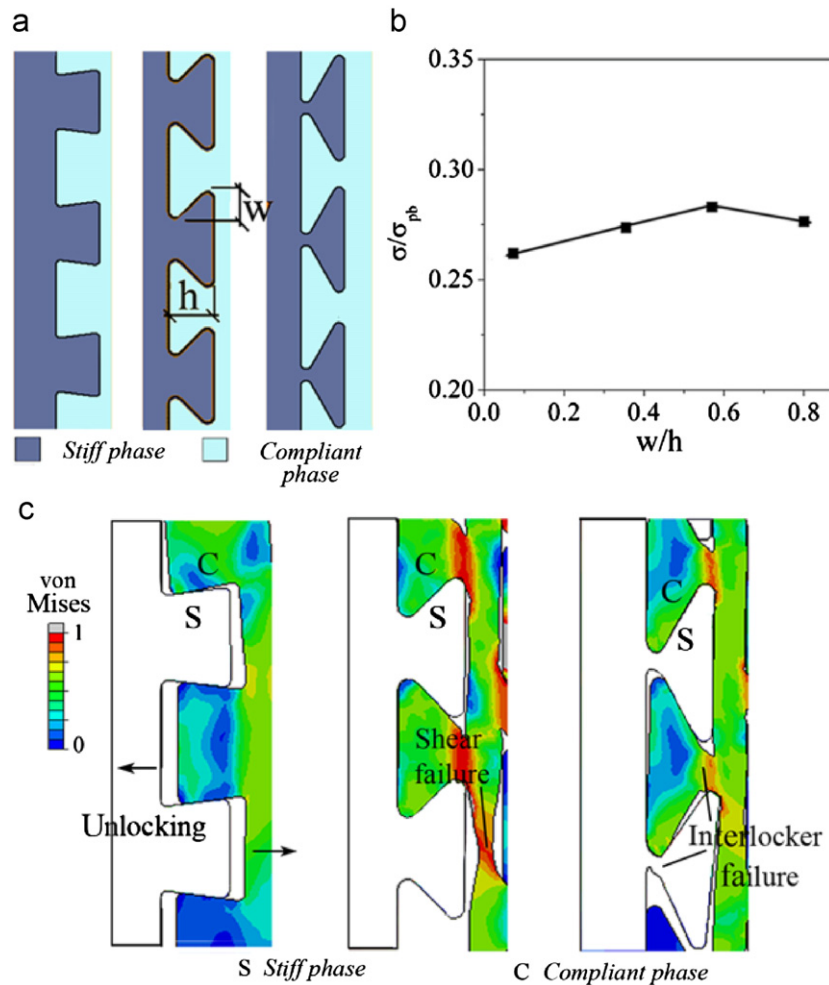

Fig. 3 – (a) Schematics of anti-trapezoid interlocker with different shoulder width w and the same shoulder height h. (b) Variation of the calculated tensile strength with the anti-trapezoid shoulder width normalized by the height; here the tensile strength is normalized by the ideal strength σ_{pb}. (c) von Mises stress field in the compliant phase for each model under the maximum sustainable load; the stress here is normalized by the yield strength of compliant phase.
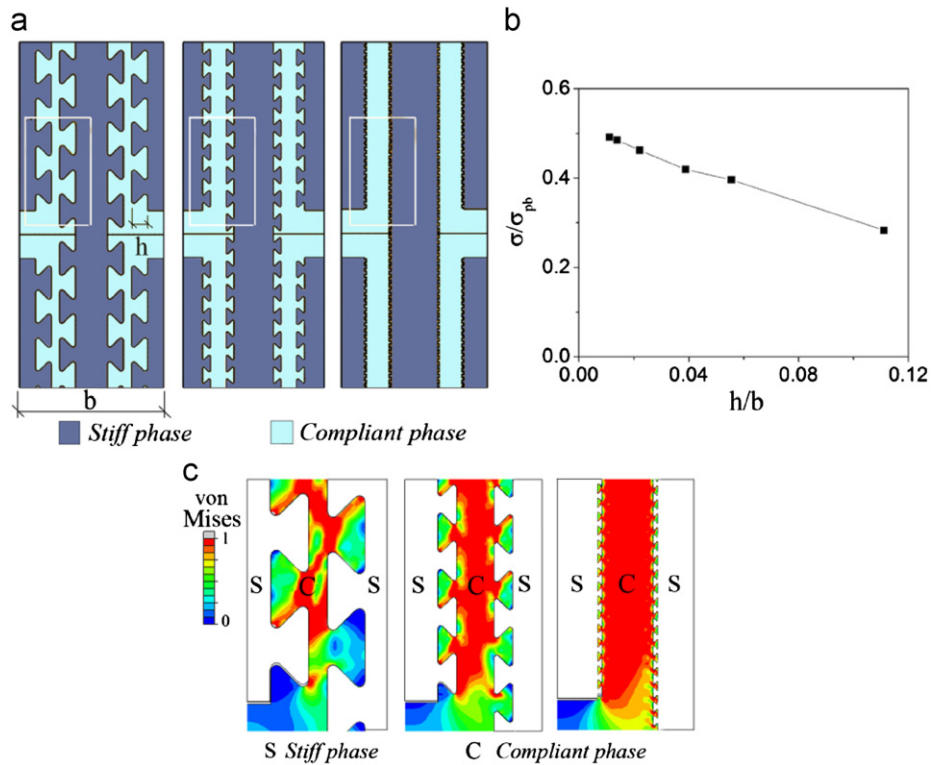
Fig. 4 – (a) Schematics of anti-trapezoid interlocker designs with different sizes. (b) Variation of the calculated tensile strength with the size of anti-trapezoid interlocker. (c) von Mises stress distributions in the regions as enclosed in (a) under respective maximum sustainable loads. Here stress is normalized by yield strength of the compliant phase.
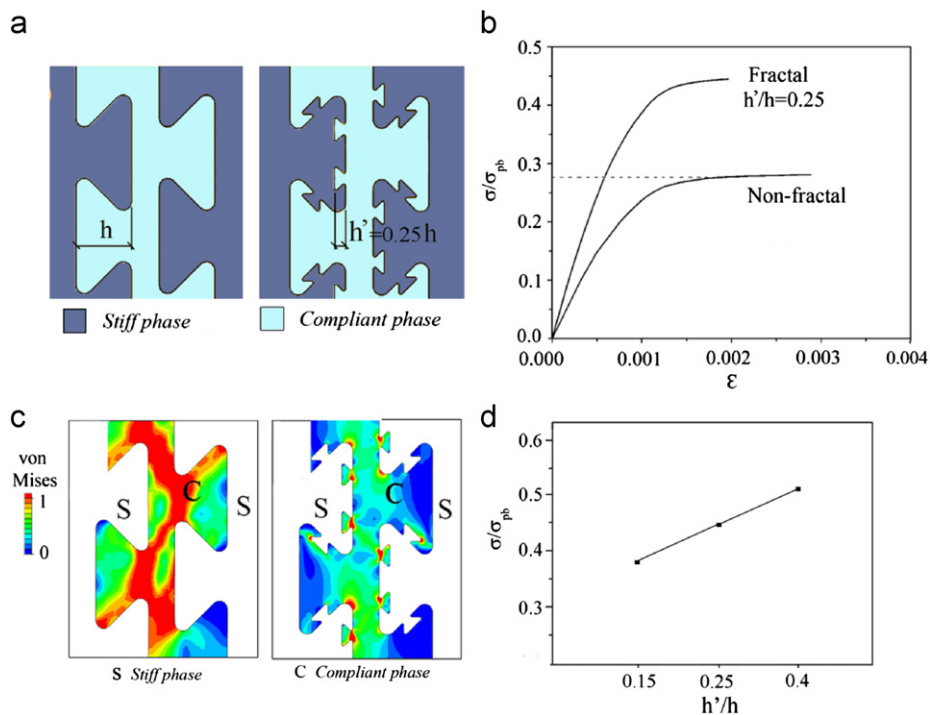

Fig. 5 – (a) Schematics of the non-fractal anti-trapezoid and the fractal anti-trapezoid designs. (b) Representative stress-strain curves for the fractal anti-trapezoid model in comparison with that for the non-fractal model. (c) von Mises stress distribution in organic material for the non-fractal and the fractal model under the same tension load as delineated by the dotted line in (b). The stress here is normalized by the yield strength of compliant phase. (d) Variation of the tensile strength with the height of the anti-trapezoid at the second order of fractal.

between the stiff and compliant phases in the lateral direction becomes loose. Under external loading, lateral unlocking of two phases will happen easily, giving rise to lower tensile strength of the composites. Among the cases we considered, the highest tensile strength is achieved when the shoulder width is taken as $0.5h$.

We proceeded further to study the effect of the anti-trapezoid size on the tensile strength. Based on the discussions above, we adopted the ratio $w/h=0.5$. By varying the anti-trapezoid height h (Fig. 4a), the effect of anti-trapezoid size on tensile strength was investigated. Fig. 4b shows the variation of the normalized tensile strength with the normalized height h/b, where b stands for the width of the unit cell as denoted in Fig. 4a. Within the range we studied ($0.011 \leq h/b \leq 0.11$), the smaller the joint size, the higher the tensile strength. The maximum strength, which reaches as high as 49% of the ideal strength σ_{pb}, is obtained when $h/b=0.011$. Such behavior of the tensile strength may be understood by observing the stress and deformation at the critical moments. Tensile yielding of the composites occurs either due to interfacial separation or yielding of the compliant material. Fig. 4c shows the stress distribution of all models at their maximum stress states. It can be seen that no obvious unlocking happens in these three cases. For the model with large anti-trapezoid size, only a small portion of compliant matrix yields and thereby the load-bearing capacities of the component materials have not been fully utilized. With decreasing interlocker size, the stress distribution in the compliant layer tends to be more homogeneous and a majority of compliant materials yield simultaneously, resulting in an increase in tensile strength of the composites. Here, we achieved half of the theoretical tensile strength just by interlocker size which is about 1/100 of the unit cell width. Based on the trend shown in Fig. 4b, it is believed that even higher tensile strength can be achieved with finer interlockers, which would incur much higher computational cost and therefore has not been attempted.

Inspired by the hieratical interlocking structures observed on the interfaces in biomaterials, we investigated the effect of hierarchy of interlocking structure on the tensile strength. Based on the anti-trapezoid model mentioned above, we created a self-similar (or fractal) anti-trapezoid model, as shown in Fig. 5a. For comparison, the hierarchy was introduced in such a way that the volume fraction of compliant/stiff materials remains unchanged. Tensile strength was explored for cases with various size ratios of h'/h, where h' is the height of the anti-trapezoid at the second order of fractal. Fig. 5b shows the calculated stress–strain curve for the fractal interlocker design with $h'/h=0.25$ in comparison to that of the corresponding non-fractal case. It can be seen that the tensile strength can be enhanced by 57% by introducing structural hierarchy on the interlocker. Fig. 5c shows the comparison of the von Mises stress field for the fractal and non-fractal cases under the same tensile load. It can be seen that the plastic zone of the non-fractal case is much larger than that of the fractal case under the same loading, implying that the fractal structure can sustain higher loading than the non-fractal one. The variation of the tensile strength with the ratio of h'/h is shown in Fig. 5d. From the cases we studied, it can be seen that larger h' results in higher tensile strength.
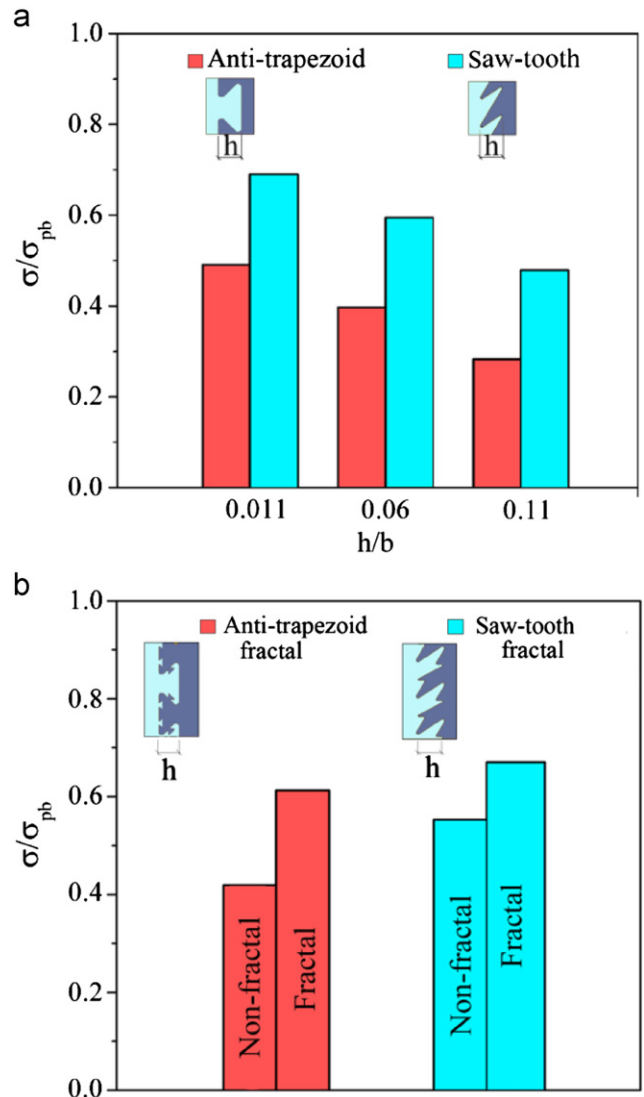

Fig. 6 – Comparison of strengthening effect between anti-trapezoid and saw-tooth designs (a) before and (b) after the incorporation of structural hierarchy. For the cases studied in (b), $h/b=0.038$.

3.2. Strengthening effects of the saw-tooth design

Besides the anti-trapezoid design discussed above, we also considered the saw-tooth interlocker design (see Fig. 6), which is also often observed in nature (Krauss et al., 2009; Saunders, 1995). In order to make a comparison with the anti-trapezoid case, we took the volume fraction of the stiff materials $\Phi=60\%$ and the normalized teeth width $w/h=0.5$ respectively. Fig. 6a shows calculated tensile strength of the saw-tooth design as a function of the normalized tooth height h/b. Like the anti-trapezoid case, Fig. 6a suggests that the saw-tooth design with lower tooth height facilitates higher tensile strength. In addition, the saw-tooth design would provide even higher tensile strength in comparison to the anti-trapezoid design with the same height. Likewise, the effect of structural hierarchy was also investigated for the saw-tooth design. As expected, structural hierarchy promotes

the tensile strength of the saw-tooth design as well, as shown in Fig. 6b. In comparison to the anti-trapezoid design, the saw-tooth design exhibits better strengthening capability no matter structural hierarchy is present or not. Our computational results show that fractal saw-tooth interlocking design can achieve tensile strength as high as 70% of the ideal value. But this does not mean that saw-tooth design is the optimal design. Other geometrical designs may exist with ability to achieve even higher tensile strength.

4.   Conclusion and discussion

In this paper, we systematically investigated the interfacial strengthening strategy for B-and-M composites through geometrically interlocking design. Our results showed that proper geometrical design of interlocker can effectively strengthen the mechanical junction between the compliant and stiff phases in the composites. As the best scenario in our results, the fractal saw-tooth interlocking design was found to be able to achieve the tensile strength of the composites up to 70% of the perfectly bonded case; in contrast, plain interfaces without any interlocking design result in zero tensile strength. The present study has mainly focused on the strengthening effect of interfacial interlocking design. It should be of equivalent importance to understand the effect of interfacial interlocking on other key mechanical properties, including energy dissipation, toughness, impact response and fatigue failure. For example, our case study also illustrates introduction of hierarchy into the interlocking designs would promote the energy dissipation by 20–25%. Detailed discussion on the other properties would be made in our future work.

In fact, mechanical interlocking, as a connection mechanism, has been used for a long time even though quantitative interpretation is little. For instance, prior to the advent of cement the ancient Chinese architects used the rivet-and-tenon structures (Fang et al., 2001) to connect the wooden components (e.g. beams and pillars) to build some of the ancient historical architectures such as the Forbidden City. Recently, mechanical interlocking has also been used in the emerging areas such as biomedical engineering and biomimetics. For instance, the connection between bone cement, a type of man-made material for bone fixation, and the spongy bone is effectively strengthened by mechanical interlocking (Mann et al., 1998; Shang et al., 2006). The roughness of ceramic surfaces was reported to enhance toughness of artificial nacre through extremely efficient energy dissipation (Launey et al., 2009). Our results presented in this paper would be of great value to the improvement of the performance of the interlocking designs in these applications.

It should be reemphasized that in our studies, we purposely excluded other strengthening mechanisms such as the inter-phase friction and adhesion caused by van der Waals interactions, electrostatic force, and chemical bonding in order to evaluate the strengthening contribution by interfacial interlocking design solely. If one or some of these mechanisms are taken into account, even higher strength is expected (Bruck et al., 2004). For example, if we incorporate the friction between the stiff and compliant phases in our simulations discussed above,
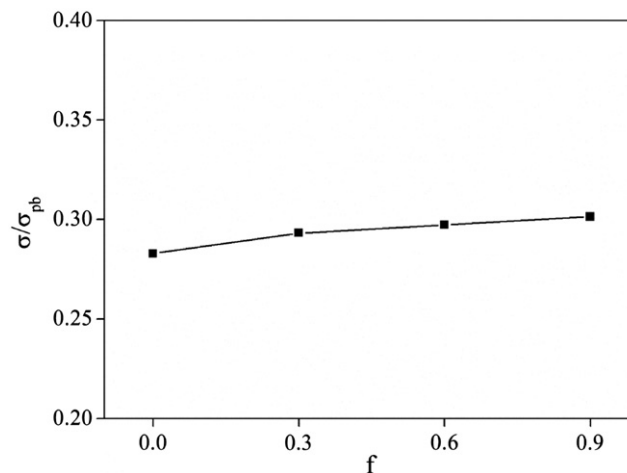

Fig. 7 – Variation of the strengthening effect with coefficient of (inter-phase) friction f for the anti-trapezoid design with $w/h=0.5$ and $h/b=0.11$.

the variation of the tensile strength with the friction coefficient is shown in Fig. 7. It is clear that friction helps promote tensile strength. To achieve even stronger interface, other mechanisms such as chemical grafting may be needed (Jackson et al., 1990; Munch et al., 2008). It should be pointed out that strong stiff/compliant interface may not always be beneficial for the mechanical performance of B-and-M composites. As we know, the operation of most toughening mechanisms in B-and-M composites, such as inter-phase friction and pullout of stiff phase from compliant phase, entails the failure of the interface between stiff and compliant phases (Clegg et al., 1990). Interface with over-high strength (e.g. perfect bonding) would prohibit the occurrence of these toughening mechanisms, giving rise to lower toughness of the composites. Therefore, high strength and high toughness raise conflicting requirements for the interface strength. There might be an optimal interfacial strength, by which high strength and high toughness could coexist in one B-and-M composite as they do in the natural biomaterials. Exploration of such optimal interfacial strength would be another topic of our future work.

Acknowledgments

REFERENCES

Bonderer, L.J., Studart, A.R., Gauckler, L.J., 2008. Bioinspired design and assembly of platelet reinforced polymer films. Science 319, 1069–1073.

Bruck, H.A., Fowler, G., Gupta, S.K., Valentine, T., 2004. Using geometric complexity to enhance the interfacial strength of heterogeneous structures fabricated in a multi-stage, multi-piece molding process. Experimental Mechanics 44, 261–271.

Clegg, W.J., Kendall, K., Alford, N.M., Button, T.W., Birchall, J.D., 1990. A simple way to make tough ceramics. Nature 347, 455–457.

Dunlop, J.W.C., Fratzl, P., 2010. Biological composites. Annual Review of Materials Research 40, 1–24.

Fang, D.P., Iwasaki, S., Yu, M.H., Shen, Q.P., Miyamoto, Y., Hikosaka, H., 2001. Ancient chinese timber architecture. I: experimental study. Journal of Structural Engineering 127, 1348.

Fratzl, P., Jager, I., 2000. Mineralized collagen fibrils: a mechanical model with a staggered arrangement of mineral particles. Biophysical Journal 79, 1737–1746.

Gao, H.J., 2006. Application of fracture mechanics concepts to hierarchical biomechanics of bone and bone-like materials. International Journal of Fracture 138, 101–137.

Gao, H.J., Ji, B.H., Jager, I.L., Arzt, E., Fratzl, P., 2003. Materials become insensitive to flaws at nanoscale: lessons from nature. Proceedings of the National Academy of Sciences of the United States of America 100, 5597–5600.

Geckeler, K.E., Rupp, F., Geis-Gerstorfer, J., 1997. Interfaces and interphases of (bio)materials: definitions, structures, and dynamics. Advanced Materials 9, 513–518.

Hammer, D.A., Tirrell, M., 1996. Biological adhesion at interfaces. Annual Review of Materials Science 26, 651–691.

Han, L., Wang, L., Song, J., Boyce, M.C., Ortiz, C., 2011. Direct quantification of the mechanical anisotropy and fracture of an individual exoskeleton layer via uniaxial compression of micropillars. Nano Letters 11, 3868–3874.

Herring, S.W., 2008. Mechanical influences on suture development and patency. Frontiers of oral biology 12, 41.

Jackson, A.P., Vincent, J.F.V., Turner, R.M., 1990. Comparison of nacre with other ceramic composites. Journal of Materials Science 25, 3173–3178.

Jasinoski, S., Reddy, B., Louw, K., Chinsamy, A., 2010. Mechanics of cranial sutures using the finite element method. Journal of Biomechanics 43, 3104–3111.

Ji, B.H., Gao, H.J., 2004. Mechanical properties of nanostructure of biological materials. Journal of the Mechanics and Physics of Solids 52, 1963–1990.

Katti, D.R., Pradhan, S.M., Katti, K.S., 2004. Modeling the organic–inorganic interfacial nanoasperities in a model bio-nanocomposite, nacre. Reviews on Advanced Materials Science 6, 162–168.

Krauss, S., Monsonego-Ornan, E., Zelzer, E., Fratzl, P., Shahar, R., 2009. Mechanical function of a complex three-dimensional suture joining the bony elements in the shell of the red-eared slider turtle. Advanced Materials 21, 407–412.

Launey, M.E., Chen, P.Y., McKittrick, J., Ritchie, R.O., 2010. Mechanistic aspects of the fracture toughness of elk antler bone. Acta Biomaterialia 6, 1505–1514.

Launey, M.E., Munch, E., Alsem, D.H., Barth, H.B., Saiz, E., Tomsia, A.P., Ritchie, R.O., 2009. Designing highly toughened hybrid composites through nature-inspired hierarchical complexity. Acta Materialia 57, 2919–2932.

Li, Y., Ortiz, C., Boyce, M., 2011. Stiffness and strength of suture joints in nature. Physical Review E 84, 062904.

Li, Y., Ortiz, C., Boyce, M.C., 2012. Bioinspired, mechanical, deterministic fractal model for hierarchical suture joints. Physical Review E 85, 031901.

Liu, B., Zhang, L., Gao, H., 2006. Poisson ratio can play a crucial role in mechanical properties of biocomposites. Mechanics of Materials 38, 1128–1142.

Mann, K.A., Allen, M.J., Ayers, D.C., 1998. Pre-yield and post-yield shear behavior of the cement-bone interface. Journal of Orthopaedic Research 16, 370–378.

Munch, E., Launey, M.E., Alsem, D.H., Saiz, E., Tomsia, A.P., Ritchie, R.O., 2008. Tough, bio-inspired hybrid materials. Science 322, 1516–1520.

Nalla, R.K., Kruzic, J.J., Ritchie, R.O., 2004. On the origin of the toughness of mineralized tissue: microcracking or crack bridging? Bone 34, 790–798.

Ortiz, C., Boyce, M.C., 2008. Materials science—bioinspired structural materials. Science 319, 1053–1054.

Podsiadlo, P., Kaushik, A.K., Arruda, E.M., Waas, A.M., Shim, B.S., Xu, J.D., Nandivada, H., Pumplin, B.G., Lahann, J., Ramamoorthy, A., Kotov, N.A., 2007. Ultrastrong and stiff layered polymer nanocomposites. Science 318, 80–83.

Rexer, J., Anderson, E., 1979. Composites with planar reinforcements (flakes, ribbons)—review. Polymer Engineering and Science 19, 1–11.

Ritchie, R.O., 2011. The conflicts between strength and toughness. Nature Materials 10, 817–822.

Saunders, W.B., 1995. The ammonoid suture problem: relationships between shell and septum thickness and suture complexity in Paleozoic ammonoids. Paleobiology 21, 343–355.

Schmidt, D., Shah, D., Giannelis, E.P., 2002. New advances in polymer/layered silicate nanocomposites. Current Opinion in Solid State and Materials Science 6, 205–212.

Shang, X., Tang, T., Dai, K., 2006. Experimental study on the shear stress of the interface between the bone and the TCP-PMMA. Journal of Medical Biomechanics 21, 111–114.

Tai, K., Dao, M., Suresh, S., Palazoglu, A., Ortiz, C., 2007. Nanoscale heterogeneity promotes energy dissipation in bone. Nature Materials 6, 454–462.

Tang, Z.Y., Kotov, N.A., Magonov, S., Ozturk, B., 2003. Nanostructured artificial nacre. Nature Materials 2, 413–U418.

Wang, L., Song, J., Ortiz, C., Boyce, M.C., 2009. Anisotropic design of a multilayered biological exoskeleton. Journal of Materials Research 24, 3477–3494.

Wang, R.Z., Suo, Z., Evans, A.G., Yao, N., Aksay, I.A., 2001. Deformation mechanisms in nacre. Journal of Materials Research 16, 2485–2493.

Weiner, S., Nudelman, F., Sone, E., Zaslansky, P., Addadi, L., 2006. Mineralized biological materials: a perspective on interfaces and interphases designed over millions of years. Biointerphases 1, 12–14.

Yao, H.M., Dao, M., Carnelli, D., Tai, K.S., Ortiz, C., 2011. Size-dependent heterogeneity benefits the mechanical performance of bone. Journal of the Mechanics and Physics of Solids 59, 64–74.

Yao, H.M., Dao, M., Imholt, T., Huang, J.M., Wheeler, K., Bonilla, A., Suresh, S., Ortiz, C., 2010. Protection mechanisms of the iron-plated armor of a deep-sea hydrothermal vent gastropod. Proceedings of the National Academy of Sciences of the United States of America 107, 987–992.